

EXPERIMENTAL INVESTIGATION OF ENHANCED SEISMIC PERFORMANCE OF STONE MASONRY USING LOW-COST RETROFIT

V. Manandhar ¹, H. Shrestha ², N. P. Marasini ³, R. Prajapati ⁴, R. Guragain ⁵, R. Chaulagain ⁶, N.
A. Alexander ⁷, F. De Luca ⁸, N. Giordano ⁹, A. G. Sextos ¹⁰

¹ National Society for Earthquake Technology – Nepal (NSET), Lalitpur, Nepal,
vibekmanandhar@nset.org.np, vibek14@gmail.com

² National Society for Earthquake Technology – Nepal (NSET), Lalitpur, Nepal

³ National Society for Earthquake Technology – Nepal (NSET), Lalitpur, Nepal

⁴ National Society for Earthquake Technology – Nepal (NSET), Lalitpur, Nepal

⁵ National Society for Earthquake Technology – Nepal (NSET), Lalitpur, Nepal

⁶ National Society for Earthquake Technology – Nepal (NSET), Lalitpur, Nepal

⁷ University of Bristol, Bristol, United Kingdom

⁸ University of Bristol, Bristol, United Kingdom

⁹ University of Bristol, Bristol, United Kingdom

¹⁰ University of Bristol, Bristol, United Kingdom

Abstract: *In the Himalayan region, stone masonry in mud mortar is a widely used typology for the construction of buildings, including schools. This is largely because of its simplicity and the materials being abundant in Nepal, where more than 80% of the land area lies in high and mid-mountainous sloping terrain. The 2015 Gorkha Earthquake revealed the severe vulnerability of stone masonry school buildings to seismic hazards, with 60% of such school buildings being damaged. There is a dire need therefore for an in-depth study on the behavior and lateral load capacity of this typology along with experimental evidence of retrofitting measures that can be implemented to make these structures resilient to earthquakes. Under the Seismic Safety and Resilience of Schools in Nepal (SAFER) project, funded by the Global Challenges Research Fund (GCRF) and the Engineering and Physical Sciences Research Council (EPSRC), UK, a series of full-scale wall tests were conducted on stone masonry walls in Kathmandu. The research made use of materials that were easily obtainable in the area, such as galvanized steel wire mesh, to retrofit walls. To understand the impact of the retrofitting in terms of load vs displacement behavior, three sets of monotonic lateral tests on stone in mud masonry walls were conducted including two non-retrofitted and four retrofitted walls using a bespoke, low-cost testing configuration. The experimental test results showed that the retrofitting intervention significantly enhanced the lateral load-bearing capacity to almost 3.5 times, while the ductility was also enhanced by a factor of 2 compared to the non-retrofitted walls. The qualitative behavior of the walls on lateral load was also observed to change. The manner in which the failure occurred underwent a transformation, with smaller and spread-out cracks replacing a larger, concentrated one. This experimental campaign emphasizes a practical and cost-effective approach for conducting seismic tests in developing countries where resources are limited, thereby contributing to the expansion of experimental data in regions with scarce resources. The study further offers significant insights into disaster risk reduction in the Himalayan region and other similar regions.*

1 Introduction

Nepal is a nation characterized by its predominantly mountainous terrain (UNDP, 2009), with 80% its populace residing in rural areas (United Nations Department of Economic and Social Affairs Population Division, 2018). One of the poorest countries in the world (IMF, 2023) and given the formidable challenges posed by the country's challenging topography, the construction of structures typically relies on locally sourced materials. According to the 2021 National census, 30% of Nepal's building stock falls under the category of low-strength load-bearing masonry (National Statistics Office, 2021). With the inherent strength and widespread availability of Stone, stone-in-mud masonry stands out as a dominant choice for construction in Nepal, a preference also adopted by educational institutions in their school building stock (De Luca *et al.*, 2019).

Nepal, with its history marked by devastating seismic events (Bilham *et al.*, 1995), holds the 11th position globally for earthquake vulnerability (United Nations Development Programme, 2009). The 2015 Gorkha Earthquake resulted in collapse of 25,134 classrooms (NPC, 2015b) and an estimated the loss of educational infrastructure and physical assets exceeding \$200 million (NPC, 2015a). According to the Structural Integrity and Damage Assessment (SIDA) report (Digicon Engineering Consult & The World Bank, 2016b) based on a study conducted in the 14 most affected districts, load Bearing Masonry schools ranked as the second most affected building typology, following steel-framed schools. The steel framed schools were also reported to have suffered major damage in their masonry infills rather than the frames. Multiple studies have demonstrated significant seismic deficiencies in a majority of masonry buildings (Brando *et al.*, 2017; Gautam & Chaulagain, 2016; Sharma *et al.*, 2016), primarily due to the involvement of owners or local laborers with limited formal training and hands-on knowledge of construction practices (Bothara & Brzev, 2012). These structures often fail to exhibit proper diaphragm behavior (Gautam *et al.*, 2016) due to sparse wall-to-wall connections between orthogonal walls and a lack of seismic detailing, including tie rods, anchors, and ring beams (Giordano *et al.*, 2019). The 2015 earthquake witnessed the most common mode of failure in masonry walls being out-of-plane displacement (Digicon Engineering Consult & The World Bank, 2016a; Lizundia *et al.*, 2016; NPC, 2015b), which poses the most serious threat to life safety (Sorrentino *et al.*, 2017).

In the quest to enhance the seismic performance of masonry structures, retrofitting strategies have been in development for an extended period. Among the prevalent methods is the application of retrofitting measures using steel Welded Wire Meshing (WWM) at strategic and critical locations. This approach comes with a cost that is roughly one third of the expense associated with reconstruction efforts (National Society for Earthquake Technology - Nepal (NSET), 2019). Nevertheless, there has been minimal exploration, both in terms of qualitative and quantitative analysis, regarding the advantages brought about by retrofitting measures when applied to stone-in-mud masonry using these techniques. The primary objective of this research was to investigate the enhancement in the lateral load behavior of stone-in-mud masonry walls through the utilization of a low-cost steel wire mesh retrofit.

2 Research on Out-of-Plane behavior of Low Strength Masonry and their Retrofit

Previous experimental campaigns have been conducted with the primary aim of comprehensively characterizing the out-of-plane behavior of masonry walls. These endeavors have involved a systematic and rigorous approach to understanding the intricate aspects of how masonry walls respond and deform when subjected to lateral forces acting perpendicular to their primary plane. Ferreira *et al.* (2015) have meticulously documented a comprehensive series of laboratory tests concerning out-of-plane behavior conducted from 1984 to 2013. These tests encompassed both static and dynamic assessments, providing invaluable insights into the evolving understanding of masonry wall behavior over the course of several decades. Further contributions to this field were made by (Doherty *et al.* (2002) affirming that out-of-plane walls exhibit greater susceptibility to displacement rather than acceleration. At the University of Adelaide, Lam *et al.* (2003) conducted a series of tests on 14 one-way regular brick unreinforced masonry (URM) wall panels, using both simple pulses and earthquake ground motions. Their study underscored the significance of response spectral displacement as a superior measure of ultimate performance compared to acceleration.

Griffith *et al.* (2007) conducted tests using eight full-scale URM walls, subjecting them to cyclic face loads with the aid of airbags. Their study highlighted the contribution of vertical pre-compression to post-peak strength and displacement capacity. Derakhshan & Ingham (2008) subjected full-scale URM walls to out-of-plane uniform static loading, emphasizing the influence of vertical pre-compression and its impact on the trilinear model shape.

Graziotti *et al.* (2016), conducted an extensive experimental campaign focused on out-of-plane shaking table tests involving cavity wall and single leaf components. In all cases, the walls exhibited one-way vertical bending/rocking failures, forming hinges at the top, bottom, and mid-height. Degli Abbati & Lagomarsino (2017) carried out both static and dynamic tests. These tests involved three models and aimed to investigate the reliability of the rigid block model in describing the rocking response of free-standing masonry elements.

In recent years, there has been a significant surge in research focused on retrofitting masonry structures. Placencia & Paredes (2017) examined the effectiveness of wire meshes and mortar in confined masonry systems for two-story Ecuadorian houses. Their study yielded positive results, demonstrating an enhancement in seismic performance. C. G. Papanicolaou *et al.* (2011) and C. G. Papanicolaou *et al.* (2008) conducted comparative studies in 2008 and 2011, assessing the efficacy of improving the out-of-plane behavior of unreinforced masonry (URM) walls through the use of Textile Reinforced Mortar (TRM) versus Fiber Reinforced Polymer (FRP). Their findings favored the use of TRM for enhancing performance. In 2014, Derakhshan *et al.* (2014) conducted an extensive in-situ out-of-plane test, showcasing the improved performance of walls following seismic enhancements and retrofitting. The study also underscored the significance of in-situ testing. Recent years have witnessed comprehensive studies exploring various materials for retrofitting and improving the out-of-plane performance of URM walls. Researchers such as Bellini *et al.* (2017) examined the use of Fiber Reinforced Cementitious Matrix (FRCM), Gattesco & Boem (2017) explored Glass Fibre Reinforced Polymer (GFRP), and De Santis *et al.* (2019) investigated Textile Reinforced Mortar (TRM). However, there remains a notable absence of dedicated research on retrofitting unreinforced stone masonry walls in mud mortar with steel Welded Wire Mesh (WWM) and the impact on the out-of-plane behavior of these walls.

3 Practice of Welded Wire Mesh (WWM) Retrofit in Nepal

In accordance with the structural design specifications, the implementation of steel Welded Wire Mesh (WWM) takes place on the specified structures. The design plan includes the incorporation of vertical splints and horizontal bandages, strategically positioned in alignment with designated openings and specific masonry segments. In other designated areas, Galvanized Iron (GI) wires are strategically spaced at greater intervals to effectively mitigate the risk of localized masonry failure and to safeguard against potential spalling of masonry units. In the process of implementing retrofitting measures utilizing steel Welded Wire Mesh (WWM) on designated structures, the following steps are followed: Initiation of the retrofitting work involves removing the existing plaster from the walls within the proposed area. Subsequently, mortar joints are carefully raked out to a depth ranging from 15-25 mm. The surface is thoroughly cleaned and moistened. The process then proceeds to excavating the soil to accommodate the tie beam or band, with reinforcement carefully laid out in this prepared trench. The application of the WWM onto the walls is executed, with the incorporation of anchor rods or through wires to securely fasten the inner and outer WWM layers to the wall. Ensuring a robust connection, the WWM is firmly anchored to the rebar of the tie beam or band. Concreting is carried out to form the tie beam or band. Following the concrete placement, plaster is applied to both the inner and outer faces of the wall. A 20mm thickness is applied to the inner face, while a 30mm thickness is employed for the outer face. This serves the dual purpose of safeguarding the mesh from corrosion and enhancing the structural integrity. The final step involves proper curing to ensure the durability and effectiveness of the retrofitting work.

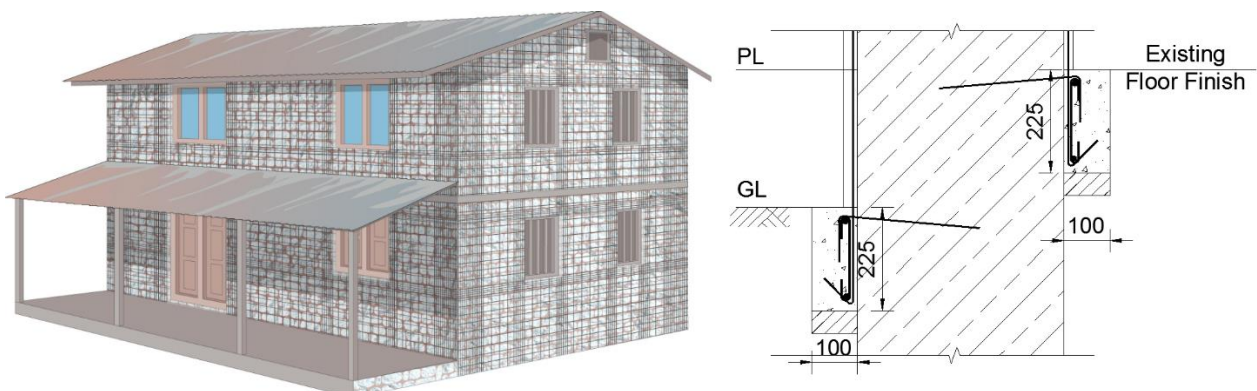


Figure 1 Typical WWM layout (left); RC tie member at the base showing through anchor rods (right)

4 Main Test

To conduct the test, a mechanism capable of consistently applying continuous and gradual deflection to the test model was devised. Subsequently, a pulldown system was designed and constructed on the premises of NSET. This system, utilizing a chain pulley for load application, was created for the purpose of the test. Precise load measurements were obtained through a digital load cell, while deflection measurements were carried out using lasers.

As the test needed to be done using semi-dressed stones, these stones were procured from the Dolakha district, located to the northeast of Kathmandu. This region was selected due to the presence of quarries offering stones with more uniform and consistent shapes. The semi-dressed

4.1 Test Walls

Both the walls were of dimension 1m (length) X 0.45m (width) X 2m (height). The width of the walls were chosen in reference to typical stone masonry schools in Nepal. The construction masons were overseen by a highly experienced head technician with extensive expertise in the construction of semi-dressed stone structures using mud mortar.

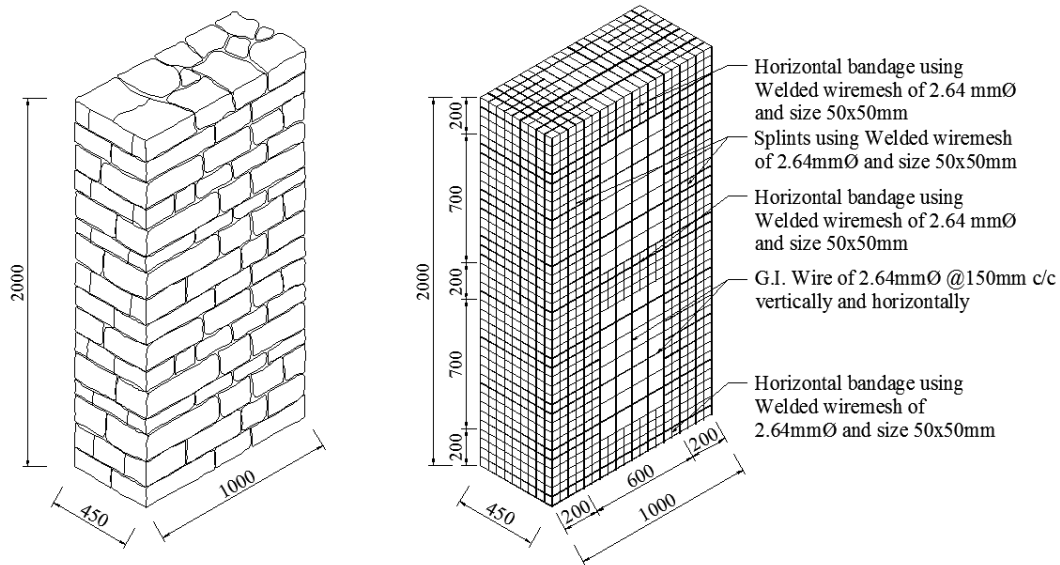


Figure 2 Isometric view of the test wall (left); WWM retrofitting detail (right)

4.2 Test Setup

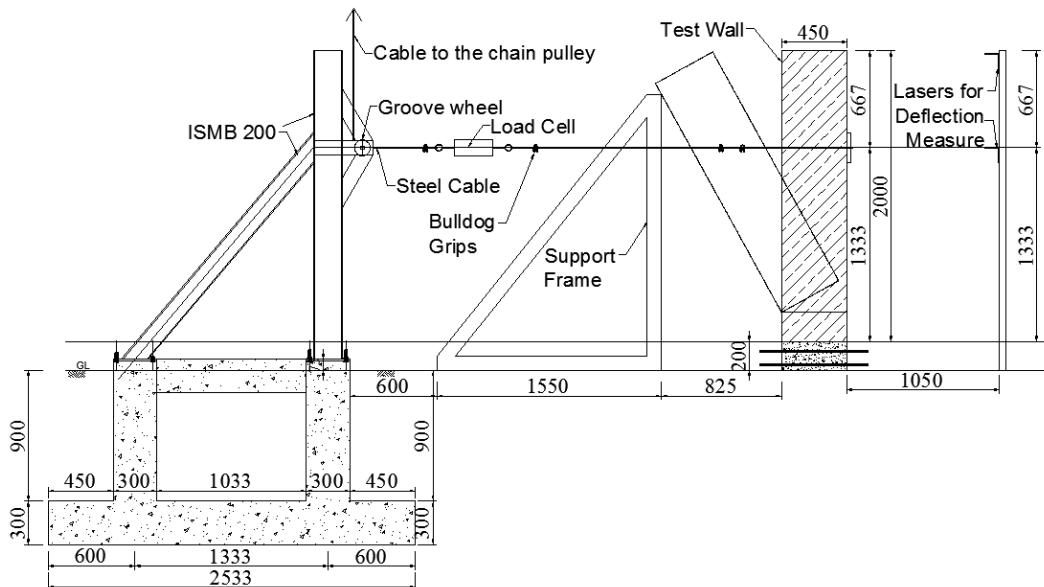


Figure 3 Setup for the latest load Pulldown test

A reinforced concrete foundation was constructed to support the reaction steel column. For the test walls, a 400mm thick raft-like stone foundation was constructed that prevented any kind of uplifting. Two M20 RC pedestals were designed to serve as a base for each wall. Multiple protruding rebar were left out for the wire mesh to be connected. To secure the pedestals to the foundation and prevent any upliftment or damage, several inverted U-shaped transverse reinforcements were provided throughout the length of the pedestals. The U shaped rebars were continued to the base of the foundation and anchored with 100mm thick M20 concrete. This comprehensive design and construction approach ensured both the stability and structural integrity of the reaction column and the pedestals.



Figure 4 Wire mesh tied and welded to the rebar of the pedestal (left); Connections covered with 50mm of 1:6 plaster (right)



Figure 5 Chain pulley arrangement (left); Pull-down setup for retrofitted wall (mid); Lasers placed pointing towards the retrofitted wall, using the non-retrofitted wall as support (right)

5 Results

The pull-down test was conducted in three distinct sets, which yielded a total of six load versus deformation curves. The initial set of walls underwent testing in January 2020, followed by the second set in August 2020, and the third set in April 2021. This sequential testing approach allowed for the collection of comprehensive data and insights regarding the behavior of the structures over time, considering various testing conditions.

5.1 First Set

The result of the test, where one of the two walls was retrofitted, are discussed below.

The retrofitted wall exhibited a maximum load capacity of 11.87KN, whereas the non-retrofitted wall exhibited a maximum load capacity of 2.8KN. The ultimate top deflection significantly improved, increasing from 281mm to 650mm as a result of the retrofitting. The load versus displacement curve, derived from the integration of load and displacement data, is presented below:

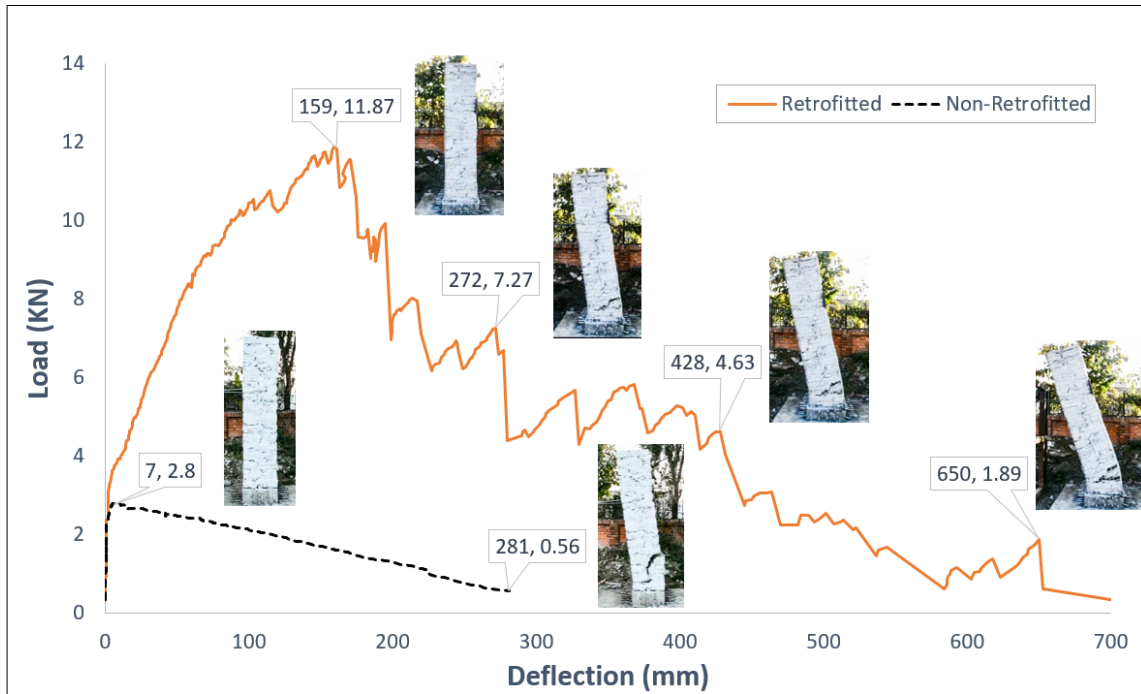


Figure 6 Load vs Displacement curves of the Retrofitted and Non-retrofitted walls of first test (pictures correspond to the top deflection and load values to their immediate left)

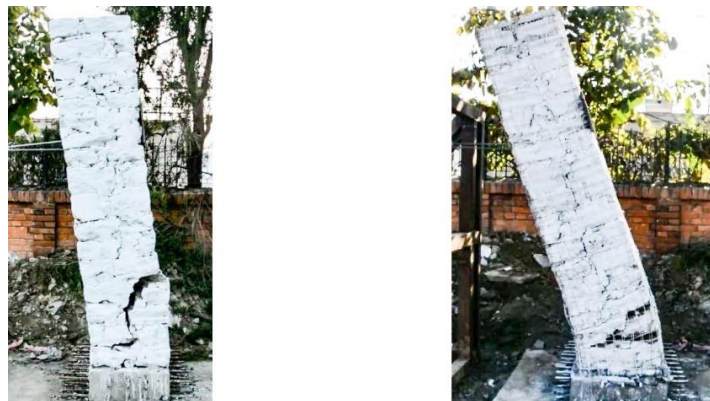


Figure 7 Final deflected shape of the non-retrofitted (left) and retrofitted (right) wall before collapse

Both walls initially displayed substantial stiffness, with both structures accommodating a load of 2.5KN within a mere 1 mm of deflection. In the case of the non-retrofitted wall, the peak load of 2.8KN was attained at a 5 mm deflection point, after which the load displacement curve followed a gradual descent. Notably, the presence of cracks was highly localized, primarily emerging on the tension side at a height of 0.5m.

As the applied load increased, the horizontal crack extended to the front-lower level, reaching the interface between the lowermost and second lowermost stone unit, as depicted in Figure 7.

For the non-retrofitted wall, the average rate of top displacement was measured at 0.87 mm/sec, and the loading increased at an average rate of 0.023KN/sec until reaching the peak load. These observations provide valuable insights into the structural behavior under load, offering essential data for analysis and evaluation.

For the retrofitted wall, a notable high stiffness persisted until a loading of 3.75KN, corresponding to a 6mm deflection. Beyond this point, there was a slight reduction in stiffness, observable until a loading of 8.25KN, equating to a 56mm deflection. The curve remained generally smooth up to this juncture, after which minor

undulations became apparent in the curve. These undulations were observed due to the displacement of stone layers occurring at the unit-mortar interface. The curve then ascended to its peak load of 11.87KN, coinciding with a deflection of 159mm. At this specific point, visible cracks had formed at a height of 0.25m, which accounts for approximately 1/8th of the wall's total height. Subsequently, the curve exhibited an overall descending trend. Within this descending portion, abrupt declines and rises were observed, corresponding to the activation of different segments of the mesh. Furthermore, sharp declines occurred when the mesh wires yielded, leading to the fracture of welds and the activation of subsequent mesh regions. Notably, the greatest degree of yielding was identified at the junction between the GI wires spaced at 150mm c/c and the lowermost horizontal band. This was evident through the fracture of the topmost horizontal wires of the bands. Ultimately, the wall reached its failure point at a top deflection of 650mm, which was associated with a load of 1.89KN. This failure resulted from the breakage of wires associated with the splints. Throughout the loading sequence, the average rate of top displacement was 1.56mm/sec, and the rate of loading increment averaged at 0.05KN/sec until the peak load was reached. These detailed observations contributed valuable insights into the behavior of the retrofitted wall under gradual increased loading.

5.2 Second Set

The second set of tests was conducted in August 2020, employing identical materials, setup, and configuration as the previous test. In an effort to introduce variability in workmanship, a distinct team of unskilled workers was engaged, albeit under the supervision of the same experienced head technician. Interestingly, the alteration in personnel did not impact the quality of workmanship, the construction timeline, or the final outcome.

The principal distinction in this test pertained to the detailing of wire anchorage. In contrast to the previous test, where the wire mesh had been welded to the protruding rebars of the pedestal, in this instance, welding was eschewed. Instead, the wire mesh was wound around the bars, securely fastened with binding wire, and enveloped with a rich plaster mix in a 1:3 ratio. This modification introduced an essential variant in the testing procedure, warranting careful consideration of its potential implications.

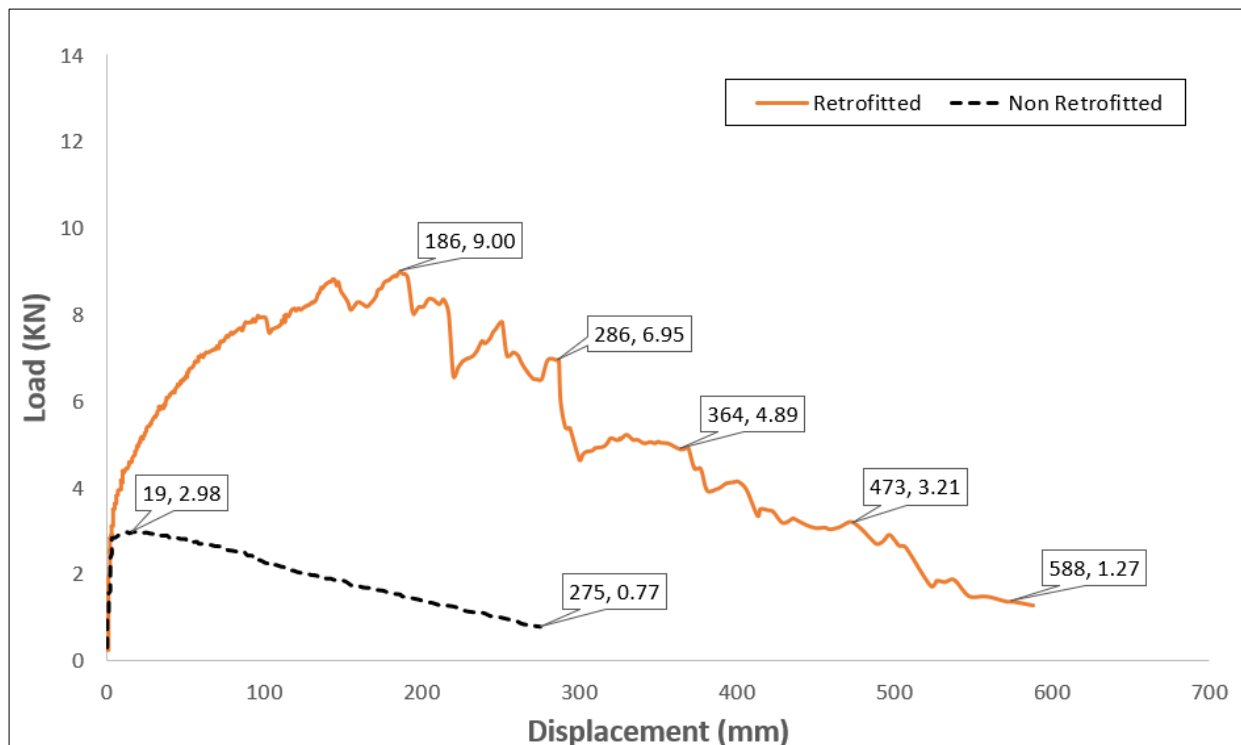


Figure 8 Load vs Displacement curves of the Retrofitted and Non-retrofitted walls of the Second Test

The retrofitted wall exhibited a maximum load of 9 KN, whereas the non-retrofitted wall registered a load of 2.98 KN. Similarly, the ultimate deflection measured 275 mm for the retrofitted wall and 588 mm for the non-retrofitted wall. The initial loading phase displayed high stiffness, and the formation and propagation of initial cracks followed a pattern similar to that observed in the first test for both retrofitted and non-retrofitted walls.

Gradual failure of welds at various sections of the wire mesh led to abrupt drops in the load vs. deformation diagram. The behavior of the non-retrofitted wall in the second test closely matched that of the first test, with only a 6.4% difference in peak load (2.98 KN in the second test vs. 2.8 KN in the first) and a 2.18% difference in ultimate deflection (275 mm in the second test vs. 281 mm in the first). However, the retrofitted wall in the second test exhibited a notable deviation, with a 24.18% lower peak load (9 KN in the second test vs. 11.87 KN in the first). This discrepancy warranted further investigation to understand the factors contributing to this difference in performance.

The main factor that could be linked to this outcome was the variation in the failure mechanism of the retrofitting element. It was noted that the wires became dislodged from their anchorage point and were unable to achieve their full capacity due to the absence of welding to the pedestal rebars. This underscores the significance of ensuring the proper anchorage of these retrofitting elements to the foundation. In practical implementation, this is typically accomplished by embedding the retrofitting element into a reinforced concrete band.

In the second set, the outcome for the retrofitted wall was found to be inconsistent with the first. Consequently, it was deemed necessary that in the next test, both walls would be retrofitted with proper anchorage at the base, akin to the retrofitted wall in the initial test. This step was primarily taken to reproduce the results achieved with the retrofitted wall, as it necessitated the consideration of additional parameters, such as the anchorage of the retrofitting elements.

5.3 Third Set

The third set of tests was conducted in April 2021, wherein both walls underwent retrofitting. The welded wire mesh was securely affixed and welded to the pedestal to prevent connection failure, mirroring the approach used for the walls in the first set. However, the connection was coated with a rich plaster mixture of 1:3. The construction masons were the same as those in the second set, but different technicians were responsible for retrofitting the walls this time. Nevertheless, the quality of the finish was maintained at the same standard as in the previous tests. The maximum loads observed were 12.48 KN and 10.29 KN, with both walls exhibiting an ultimate deflection exceeding 600mm, specifically 610mm and 694mm. While there was a difference in peak load resistance between the two walls, the energy absorbed by them was nearly equal, as illustrated in the figure below.

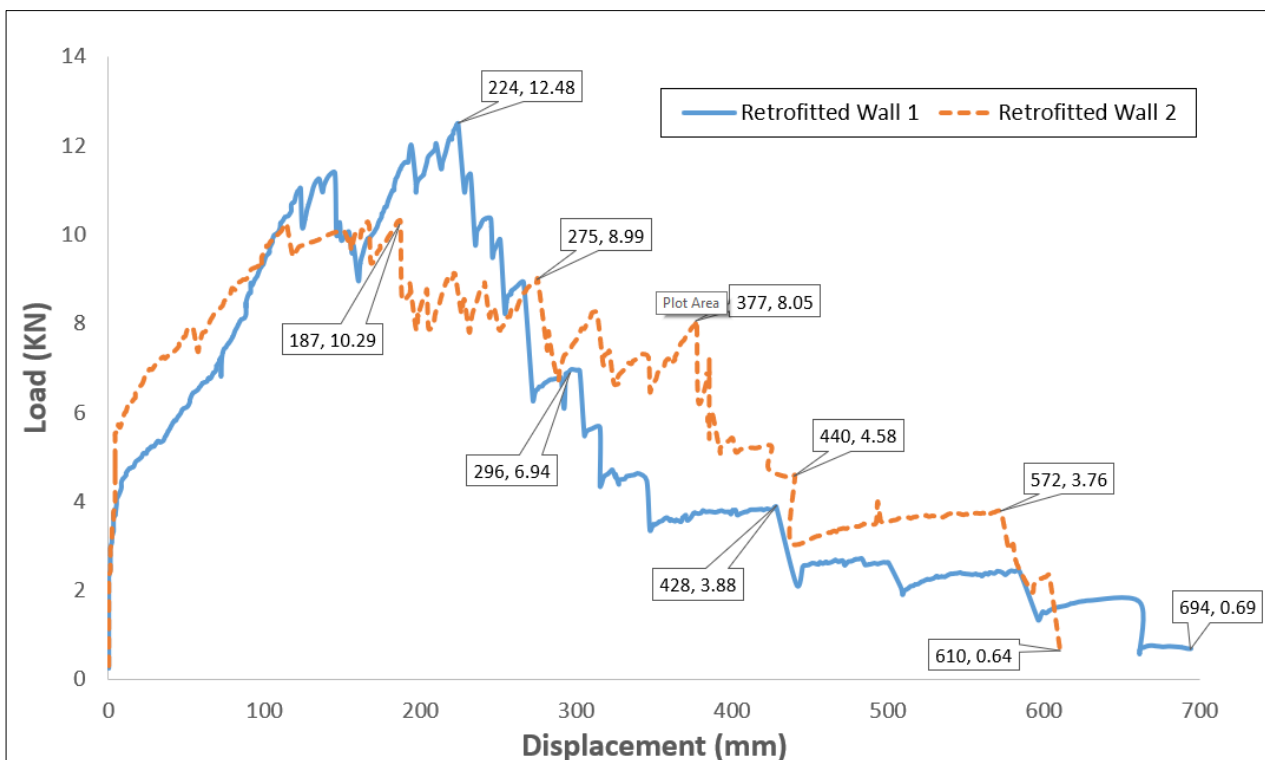


Figure 9 Load vs Displacement curves of the two retrofitted walls of the Third Test

The second wall, which had a peak load of 10.29 KN, ultimately performed more work, totaling 3993.71 KNmm. In contrast, the first wall, with a peak load of 12.48 KN, completed 3745.26 KNmm of work (6.22% less). Both walls were found to absorb comparable amounts of energy, despite having different peak loads. Additionally, the failure mode observed in these walls was consistent with what was observed in previous tests. It was concluded that in both walls, the wire meshes failed due to rupture, rather than experiencing anchorage failure at the base.

The distinction in the characteristics of the curves for the two retrofitted walls in the last test also demonstrates how the lateral load plot, depicting the behavior of masonry walls, can vary, despite all physical parameters and failure patterns of the two walls being essentially identical.

6 Conclusion

Lateral load tests were conducted on non-retrofitted and retrofitted stone in mud masonry walls, using semi dressed stones in mud mortar. These walls were representative of typical Nepali construction found in both residential and educational buildings. The results revealed that retrofitting stone in mud walls with Welded Wire Mesh (WWM) had a significant positive impact on both the lateral load capacity and deformability in all the tests. This intervention, which costs less than a third of the expenses required for reconstructing the same structure, demonstrated compelling outcomes.

In summary, the retrofitted walls exhibited a peak load capacity at least 3.45 times greater than that of the non-retrofitted walls, considering the highest observed peak load value among non-retrofitted walls (2.98 KN) and the lowest observed value among retrofitted walls (10.29 KN). Additionally, retrofitting improved the ultimate deflection to at least two times the value observed in non-retrofitted walls, considering the maximum ultimate deformation value among non-retrofitted walls (282mm) and the lowest ultimate deformation value among retrofitted walls (572mm). It was noted that the drying duration, which varied between 53 days, 18 days, and 237 days for the first, second, and third set of walls respectively, did not significantly affect the lateral load behaviour of the walls.

Additionally, this study underscores a practical approach for conducting cost-effective tests in developing country contexts, paving the way for expanding the knowledge base on low-strength masonry through further experimental investigations in these regions.

Further avenues of research can be testing of other typologies like dry stone and dressed stone masonry walls. The confining effect of plaster that can cater to a more uniform activation of the mesh can also be explored. Other possible cost-effective methods and retrofit techniques using locally available materials can also be studied.

7 Acknowledgements

This work was done as a part of the SAFER (Seismic Safety and Resilience of Schools in Nepal) project. It is a holistic and multi-disciplinary program for improving the earthquake-related safety of school buildings and the resilience of educational communities in Nepal led by University of Bristol, UK. The author acknowledges the cooperation of Institute of Engineering, Tribhuvan University, Nepal for the pilot tests and all the supporting personnel of the project for contributing to the overall operation of the campaign.

8 References

- Bellini, A., Incerti, A., Bovo, M., & Mazzotti, C. (2017). Effectiveness of FRCM Reinforcement Applied to Masonry Walls Subject to Axial Force and Out-Of-Plane Loads Evaluated by Experimental and Numerical Studies. *International Journal of Architectural Heritage*, 12(3), 376–394.
<https://doi.org/10.1080/15583058.2017.1323246>
- Bilham, R., Bodin, P., & Jackson, M. (1995). Entertaining a great earthquake in western Nepal: Historic inactivity and geodetic tests for the present state of strain. *Journal of Nepal Geological Society*, 11(1), 73–78.
- Bothara, J., & Brzev, S. (2012). A Tutorial: Improving the Seismic Performance of Stone Masonry Buildings. In *World Housing Encyclopaedia* (Issue July).

- Brando, G., Rapone, D., Spacone, E., O'Banion, M. S., Olsen, M. J., Barbosa, A. R., Faggella, M., Gigliotti, R., Liberatore, D., Russo, S., Sorrentino, L., Bose, S., & Stravidis, A. (2017). Damage Reconnaissance of Unreinforced Masonry Bearing Wall Buildings After the 2015 Gorkha, Nepal, Earthquake. *Earthquake Spectra*, 33(Special issue 1), S243–S273. <https://doi.org/10.1193/010817EQS009M>
- De Luca, F., Giordano, N., Gryc, H., Hulme, L., McCarthy, C., Sanderson, V., & Sextos, A. (2019, April). *Nepalese School Building Stock and Implications on Seismic Vulnerability Assessment*. <https://www.researchgate.net/publication/334697946>
- De Santis, S., De Canio, G., de Felice, G., Meriggi, P., & Roselli, I. (2019). Out-of-plane seismic retrofitting of masonry walls with Textile Reinforced Mortar composites. *Bulletin of Earthquake Engineering*, 17(11), 6265–6300. <https://doi.org/10.1007/s10518-019-00701-5>
- Degli Abbati, S., & Lagomarsino, S. (2017). Out-of-plane static and dynamic response of masonry panels. *Engineering Structures*, 150, 803–820. <https://doi.org/10.1016/j.engstruct.2017.07.070>
- Derakhshan, H., Dizhur, D., Griffith, M. C., & Ingham, J. M. (2014). In situ out-of-plane testing of as-built and retrofitted unreinforced masonry walls. *Journal of Structural Engineering (United States)*, 140(6). [https://doi.org/10.1061/\(ASCE\)ST.1943-541X.0000960](https://doi.org/10.1061/(ASCE)ST.1943-541X.0000960)
- Derakhshan, H., & Ingham, J. (2008). Out-of-Plane testing of an unreinforced masonry wall subjected to one-way bending. *Australian Earthquake Engineering ...*, NOVEMBER 2008.
- Digicon Engineering Consult, & The World Bank. (2016a). *Structural Integrity and Damage Assessment: PHASE I RESULTS AND FINDINGS*.
- Digicon Engineering Consult, & The World Bank. (2016b). *Structural Integrity and Damage Assessment (SIDA) - Phase I*.
- Doherty, K., Griffith, M. C., Lam, N., & Wilson, J. (2002). Displacement-based seismic analysis for out-of-plane bending of unreinforced masonry walls. *Earthquake Engineering and Structural Dynamics*, 31(4), 833–850. <https://doi.org/10.1002/eqe.126>
- Ferreira, T. M., Costa, A. A., & Costa, A. (2015). Analysis of the Out-Of-Plane Seismic Behavior of Unreinforced Masonry: A Literature Review. *International Journal of Architectural Heritage*, 9(8), 949–972. <https://doi.org/10.1080/15583058.2014.885996>
- Gattesco, N., & Boem, I. (2017). Out-of-plane behavior of reinforced masonry walls: Experimental and numerical study. *Composites Part B: Engineering*, 128, 39–52. <https://doi.org/10.1016/j.compositesb.2017.07.006>
- Gautam, D., & Chaulagain, H. (2016). Structural performance and associated lessons to be learned from world earthquakes in Nepal after 25 April 2015 (MW 7.8) Gorkha earthquake. *Engineering Failure Analysis*, 68, 222–243. <https://doi.org/10.1016/j.engfailanal.2016.06.002>
- Gautam, D., Rodrigues, H., Bhetwal, K. K., Neupane, P., & Sanada, Y. (2016). Common structural and construction deficiencies of Nepalese buildings. *Innovative Infrastructure Solutions*, 1(1). <https://doi.org/10.1007/s41062-016-0001-3>
- Giordano, N., De Luca, F., Sextos, A., & Maskey, P. N. (2019). Derivation of fragility curves for URM school buildings in Nepal. *13th International Conference on Applications of Statistics and Probability in Civil Engineering, ICASP 2019*.
- Graziotti, F., Tomassetti, U., Penna, A., & Magenes, G. (2016). Out-of-plane shaking table tests on URM single leaf and cavity walls. *Engineering Structures*, 125(October), 455–470. <https://doi.org/10.1016/j.engstruct.2016.07.011>
- Griffith, M. C., Vaculik, J., Lam, N. T. K., Wilson, J., & Lumantarna, E. (2007). Cyclic testing of unreinforced masonry walls in two-way bending. *Earthquake Engineering and Structural Dynamics*, 36(6), 801–821. <https://doi.org/10.1002/eqe.654>
- IMF. (2023). *WORLD ECONOMIC OUTLOOK, APRIL 2023*. INTL MONETARY FUND.

- Lam, N. T. K., Griffith, M., Wilson, J., & Doherty, K. (2003). Time-history analysis of URM walls in out-of-plane flexure. *Engineering Structures*, 25(6), 743–754. [https://doi.org/10.1016/S0141-0296\(02\)00218-3](https://doi.org/10.1016/S0141-0296(02)00218-3)
- Lizundia, B., Shrestha, S. N., Bevington, J., Davidson, R. A., Jaiswal, K., Jimée, G. K., Kaushik, H. B., Kumar, H., Kupec, J., Mitrani-Reiser, J., Poland, C. D., Shrestha, S., Welton-Mitchell, C., Tremayne, H., & Ortiz-Milan, M. (2016). *EERI earthquake reconnaissance team report: M7.8 Gorkha, Nepal Earthquake on April 25, 2015 and its aftershocks*. Earthquake Engineering Research Institute.
- National Society for Earthquake Technology - Nepal (NSET). (2019). *A Report on Implementation of "Training on Retrofitting of Masonry Buildings for Existing Masons."*
- National Statistics Office. (2021). *National Population and Housing Census 2021*. www.cbs.gov.np
- NPC. (2015a). *Nepal Earthquake 2015 Post Disaster Needs Assessment (Vol A)*.
- NPC. (2015b). *Nepal Earthquake 2015 Post Disaster Needs Assessment (Vol B)*. www.npc.gov.np
- Papanicolaou, C. G., Triantafillou, T. C., Papatthanasidou, M., & Karlos, K. (2008). Textile reinforced mortar (TRM) versus FRP as strengthening material of URM walls: Out-of-plane cyclic loading. *Materials and Structures/Materiaux et Constructions*, 41(1), 143–157. <https://doi.org/10.1617/s11527-007-9226-0>
- Papanicolaou, C., Triantafillou, T., & Lekka, M. (2011). Externally bonded grids as strengthening and seismic retrofitting materials of masonry panels. *Construction and Building Materials*, 25(2), 504–514. <https://doi.org/10.1016/j.conbuildmat.2010.07.018>
- Placencia, P., & Paredes, P. (2017). Wire-Mesh and Mortar Confined Masonry As Seismic Resistant System for Houses Up To Two Stories. *16th World Conference on Earthquake*, 1–12.
- Sharma, K., Deng, L., & Noguez, C. C. (2016). Field investigation on the performance of building structures during the April 25, 2015, Gorkha earthquake in Nepal. *Engineering Structures*, 121, 61–74. <https://doi.org/10.1016/j.engstruct.2016.04.043>
- Sorrentino, L., D'Ayala, D., de Felice, G., Griffith, M. C., Lagomarsino, S., & Magenes, G. (2017). Review of Out-of-Plane Seismic Assessment Techniques Applied To Existing Masonry Buildings. *International Journal of Architectural Heritage*, 11(1), 2–21. <https://doi.org/10.1080/15583058.2016.1237586>
- UNDP. (2009). *NEPAL COUNTRY REPORT - GLOBAL ASSESSMENT OF RISK, ISDR Global Assessment Report on Poverty and Disaster Risk 2009*. <http://www.undp.org.np>
- United Nations Department of Economic and Social Affairs Population Division. (2018). *World Urbanization Prospects The 2018 Revision*.
- United Nations Development Programme. (2009). *Nepal Country Report: Global Assessment Risk*.